NEOPLASIA
www.neoplasia.com

Volume 15 Number 5 May 2013 pp. 523–534 523

Inauhzin Sensitizes p53-Dependent Cytotoxicity and Tumor Suppression of Chemotherapeutic Agents[1,2]

Yiwei Zhang, Qi Zhang, Shelya X. Zeng, Qian Hao and Hua Lu

Department of Biochemistry and Molecular Biology and Tulane Cancer Center, Tulane University School of Medicine, New Orleans, LA

Abstract

Toxicity and chemoresistance are two major issues to hamper the success of current standard tumor chemotherapy. Combined therapy of agents with different mechanisms of action is a feasible and effective means to minimize the side effects and avoid the resistance to chemotherapeutic drugs while improving the antitumor effects. As the most essential tumor suppressor, p53 or its pathway has been an attractive target to develop a new type of molecule-targeting anticancer therapy. Recently, we identified a small molecule, Inauhzin (INZ), which can specifically activate p53 by inducing its deacetylation. In this study, we tested if combination with INZ could sensitize tumor cells to the current chemotherapeutic drugs, cisplatin (CIS) and doxorubicin (DOX). We found that compared with any single treatment, combination of lower doses of INZ and CIS or DOX significantly promoted apoptosis and cell growth inhibition in human non–small lung cancer and colon cancer cell lines in a p53-dependent fashion. This cooperative effect between INZ and CIS on tumor suppression was also confirmed in a xenograft tumor model. Therefore, this study suggests that specifically targeting the p53 pathway could enhance the sensitivity of cancer cells to chemotherapeutic agents and markedly reduce the doses of the chemotherapy, possibly decreasing its adverse side effects.

Neoplasia (2013) 15, 523–534

Introduction

The modern chemotherapy of cancers, which mainly refers to genotoxic/cytotoxic drugs [1], started around 1940s and has developed into several types, including alkylating agents, anthracyclines, plant alkaloids, topoisomerase inhibitors, and antimetabolites. Most of the above chemotherapeutic drugs inhibit tumor growth by causing DNA damages, arresting DNA replication, and cell division. As the representatives of alkylating agents and anthracyclines, respectively, cisplatin (CIS) and doxorubicin (DOX) are among the most potent drugs to fight against many kinds of hematologic malignancies and solid tumors [2,3]. Unfortunately, the dosage and treatment duration of these drugs, which are essential for maximizing their antitumor effects, are often limited due to severe toxicities to normal tissues, such as CIS caused nephrotoxicity and DOX caused cardiomyopathy [3–8]. These detrimental effects are usually cumulative, dose-dependent, and irreversible [5,8]. Besides toxicity, chemoresistance is another major obstacle for effective cancer chemotherapy [9]. This can result from spontaneous mutations occurring at the rate of 1 of 10^5 cells and be obtained inevitably with cell proliferation. However, resistance to two drugs occurs much less frequently (fewer than 1 in 10^{10} cells) [1]. Therefore, combined therapy using agents with different mechanisms of action and resistance has become an intriguing and promising strategy to overcome side effects and drug resistance as well as to obtain synergistic efficiency [1].

New strategies targeting aberrant pathways, dysregulated signaling molecules in tumors, and tumor-specific antigens have been developed during the past decade [1]. The tumor suppressor p53 is essentially important for preventing mammalian cells from undergoing neoplasia and tumorigenesis, primarily due to its ability to activate the transcription of numerous genes and some miRNA responsible for executing p53-dependent apoptosis, autophagy, senescence, and DNA repair as well as suppression of cell proliferation, growth, migration, and angiogenesis [10–12]. About half of human tumors contain a mutation or deletion of the *TP53* gene [13–15], and the tumors retaining wild-type p53 usually

Address all correspondence to: Hua Lu, PhD, 3181 SW Sam Jackson Park Road, Portland, OR 97239. E-mail: hlu2@tulane.edu

[1]This work was partially supported by National Institutes of Health-National Cancer Institute grants CA127724, CA095441, and CA129828 to H.L.

[2]This article refers to supplementary materials, which are designated by Figures W1 to W3 and are available online at www.neoplasia.com.

Received 7 January 2013; Revised 15 February 2013; Accepted 15 February 2013

DOI 10.1593/neo.13142

have other aberrations in their p53 pathway, such as amplified expression of MDM2 and/or MDMX [16]. MDM2 and MDMX are two physiological repressors of p53, which inactivate the latter by directly inhibiting its transcriptional activity and mediating its ubiquitination in a feedback fashion, as they are also the transcriptional targets of p53 [17–24]. On account of the importance of the p53-MDM2/MDMX pathway in the initiation and development of wild-type p53-containing tumors, intensive studies over the past decade have been aiming to identify small molecules that could specifically target individual protein molecules of this pathway for developing a better molecule-targeting anticancer therapy [25]. Several small molecules or peptides have been reported to activate p53 by either blocking its binding to MDM2 [26–28], inhibiting MDM2 E3 ubiquitin ligase activity [29], or inhibiting MDMX-p53 binding [30]. Activating p53 by targeting its deacetylase(s) is another new strategy. p53 acetylation by p300/CREB-binding protein (CBP) and ubiquitination by MDM2 are mutually exclusive [31–35], so increased acetylation could attenuate, yet increased deacetylation could facilitate, MDM2-mediated p53 ubiquitination and degradation [32,34,35]. On the basis of the high expression level of SIRT1, an enzyme to catalyze deacetylation of p53, in a number of human cancers [36–38], several inhibitors of SIRT1 [39], including Inauhzin (INZ) by our group [16], were identified to stop MDM2-mediated p53 degradation and induce p53 activation. Therefore, indirectly interrupting the MDM2-p53 negative feedback loop by inhibiting SIRT1 activity to enhance p53 acetylation could serve as an alternative strategy for the development of anticancer therapy.

Activation of the p53 signaling pathway is one of the central mechanisms for most of the genotoxic drugs to suppress tumor growth, while silence of p53 can lead to chemoresistance [40–43]. Restoring and maximizing p53 activity in tumor cells through combination of various means could be a favorable strategy to enhance the sensitivity and reduce the toxicity of chemotherapy. INZ, as a specific activator of the p53 pathway, bypassing DNA damage with retaining antitumor activity and exerting a minimal effect on the cell viability of normal human cells [16], was hypothesized to present an advantage to increase p53 activity and enhance tumor suppression, meanwhile lowering the toxicity to normal tissues and drug resistance by combination with lower dose of chemotherapeutic drugs. In our previous study [44], we demonstrated the synergistic effects of combining INZ and Nutlin-3, an inhibitor targeting the MDM2-p53 interaction [26], on p53 activation and tumor suppression. Here, we further tested the combined antitumor effects of INZ and current first-line chemotherapeutic drugs, CIS and DOX, using cell-based assays and a xenograft tumor model system. As a result, we found that the combination of two compounds at much lower doses synergistically activates p53 and induces the proapoptotic activity in human lung and colon cancer cell lines. We also observed the enhanced growth suppression of xenografted lung cancer with combination of INZ and CIS at lower doses. Therefore, this study suggests that INZ, as a new-type non-genotoxic antitumor drug candidate, could serve as a potent component of the combined therapy to improve the antitumor effects, combat the drug resistance, and reduce the side effects of chemotherapeutic drugs.

Materials and Methods

Chemicals and Antibodies

INZ was purchased from ChemDiv (San Diego, CA) or ChemBridge (San Diego, CA) and dissolved with DMSO to a concentration of 50 mM and stored at −20°C. CIS and DOX were purchased from Sigma (St Louis, MO) and dissolved with ddH_2O to a concentration of 10 mM and stored at −20°C. Cell Counting Kit was purchased from Dojindo Molecular Technologies, Inc (Gaithersburg, MD). Fluorescein *In Situ* Apoptosis Detection Kit was from Roche (Indianapolis, IN). Antibodies for Western blot (WB) included rabbit polyclonal anti-p53 (FL-393; Santa Cruz Biotechnology, Dallas, TX), rabbit polyclonal anti-p21 (M19; Santa Cruz Biotechnology), mouse monoclonal anti-p21 (CP74; NeoMarkers, Fremont, CA), mouse monoclonal anti-p21 (F-5; Santa Cruz Biotechnology), rabbit polyclonal anti-cleaved poly (ADP-ribose) polymerase (PARP) (9542 Cell Signaling Technology, Danvers, MA), and mouse anti–β-actin (Santa Cruz Biotechnology). Mouse monoclonal anti-5-bromo-2′-deoxyuridine (BrdU) antibodies (IIB5; Santa Cruz Biotechnology) were used for immunofluorescence staining.

Cell Culture

Human non–small cell lung carcinoma wild-type p53-containing H460 and A549, human non–small cell lung carcinoma p53-null H1299, human colon cancer HCT116 ($p53^{+/+}$ and $p53^{-/-}$), and normal human fibroblast cell line NHF-1 were maintained in Dulbecco's modified Eagle's medium (Gibco BRL, Carlsbad, CA) supplemented with 10% FBS and Penicillin-Streptomycin antibiotic mixture (10 ml/l; Gibco BRL) at 37°C in an incubator containing humidified air with 5% CO_2.

WB Analysis

H460, A549, H1299, and HCT116 cells cultured in six-well culture plates were grown to 80% confluence and then treated with various concentrations of INZ together with or without CIS or DOX for indicated time periods. After being washed with ice-cold phosphate-buffered saline (PBS) three times, cells were lysed with 70 μl of ice-cold lysis buffer containing 150 mM NaCl, 50 mM Tris-HCl (pH 8.0), 5 mM EDTA, 0.5% NP-40, 1 mM DTT, 0.2 mM PMSF, 0.3 μM aprotinin, 130 μM bestatin, 1 μM leupeptin, and 1 μg/ml pepstatin A. Tumor tissues from the control and treatment groups saved in liquid nitrogen were rinsed in precooled PBS, minced, and homogenized on ice with a Dounce homogenizer in RIPA lysis buffer [150 mM NaCl, 1.0% Triton X-100, 0.5% sodium deoxycholate, 0.1% sodium dodecyl sulfate, 50 mM Tris (pH 7.5), 1 mM DTT, 0.2 mM PMSF, 0.3 μM aprotinin, 130 μM bestatin, 1 μM leupeptin, and 1 μg/ml pepstatin A]. After incubation at 4°C for 30 minutes, cell or tumor tissue lysates were obtained by centrifugation at 18,000*g* at 4°C for 15 minutes, and the concentration of total protein was determined by the Bradford method. Equal amounts (50 μg per lane) of proteins obtained as described above were loaded to each lane and ran in a sodium dodecyl sulfate–polyacrylamide gel electrophoresis gel and transferred onto a nitrocellulose membrane (Bio-Rad, Hercules, CA) using a semidry transfer apparatus (Bio-Rad). After blocking in 5% nonfat dry milk in 1× TBS containing 0.1% Tween 20 (TBST) at room temperature for 1 hour, membranes were incubated with primary antibodies in the blocking buffer at 4°C overnight, followed by three washes in TBST and incubation with secondary HRP-conjugated antibody (Bio-Rad) at room temperature for 1 hour. After three washes in TBST, blots were detected with SuperSignal West Pico chemiluminescent substrate (Pierce Biotechnology Inc, Rockford, IL) and developed using Kodak Biomax film (PerkinElmer, Norwalk, CT). All blots were normalized against β-actin as a loading control.

Cell Viability Assay and Assessment of Combined Drug Effect

To assess cell growth, the Cell Counting Kit (Dojindo Molecular Technologies, Inc) was used according to the manufacturer's instructions. Briefly, cells (5000/100 μl per well) were seeded in 96-well flat-bottom plates, incubated overnight at 37°C, then treated with each compound individually at serial dilutions or both compounds simultaneously at serial dilutions with fixed molar drug ratios (INZ/CIS = 1:2 for H460 cells, INZ/CIS = 1:7 for HCT116$^{p53+/+}$, and INZ/DOX = 20:1 for H460 and HCT116$^{p53+/+}$). After treatment for 72 hours, WST-8 was added to each well at a final concentration of 10%, and the absorbance of the samples was recorded at 450 nm on a microplate reader (Molecular Devices, Sunnyvale, CA; SpectraMax M5e) after 3 hours of incubation at 37°C. The dose-effect curves were generated for each treatment to estimate the individual fractional survival (f).

The combination index (CI) values were calculated to determine the combined effects of INZ and CIS or DOX, based on the dose-effect curves obtained above, according to the following formula as previously developed [45]:

$$CI = (D)_1 / (D_f)_1 + (D)_2 / (D_f)_2 + \alpha\,(D)_1(D)_2 / (D_f)_1(D_f)_2.$$

In this formula, $(D)_1$ and $(D)_2$ are the concentrations of each compound of combination required to produce the fraction (f), $(D_f)_1$ and $(D_f)_2$ are the concentrations of individuals required to produce f, and α = 1 or 0 depending on whether the drugs are assumed to be mutually nonexclusive or mutually exclusive, respectively. In this method, CI < 1, =1, or >1 indicate synergism, additivity, or antagonism, respectively [45].

Cell Apoptosis Analysis by Flow Cytometry

Cells (1.5×10^5) were plated into six-well plates and incubated at 37°C overnight. After treatment of INZ and CIS or DOX at the indicated concentrations for 48 hours, cells were harvested, fixed in 70% ice-cold ethanol overnight at −20°C, resuspended in propidium iodide (PI) solution (50 μg/ml PI, 0.1 mg/ml RNase A, 0.05% Triton X-100 in PBS) for 40 minutes at 37°C, then analyzed for DNA content using a flow cytometer (FACSCalibur; Becton Dickinson, Franklin Lakes, NJ) and proprietary software (ModFit LT; Verity Software House, Topsham, ME).

In Vivo *Studies*

Five-week-old female SCID mice were purchased from *In vivo* Therapeutics Core, Indiana University Simon Cancer Center (Indianapolis, IN).

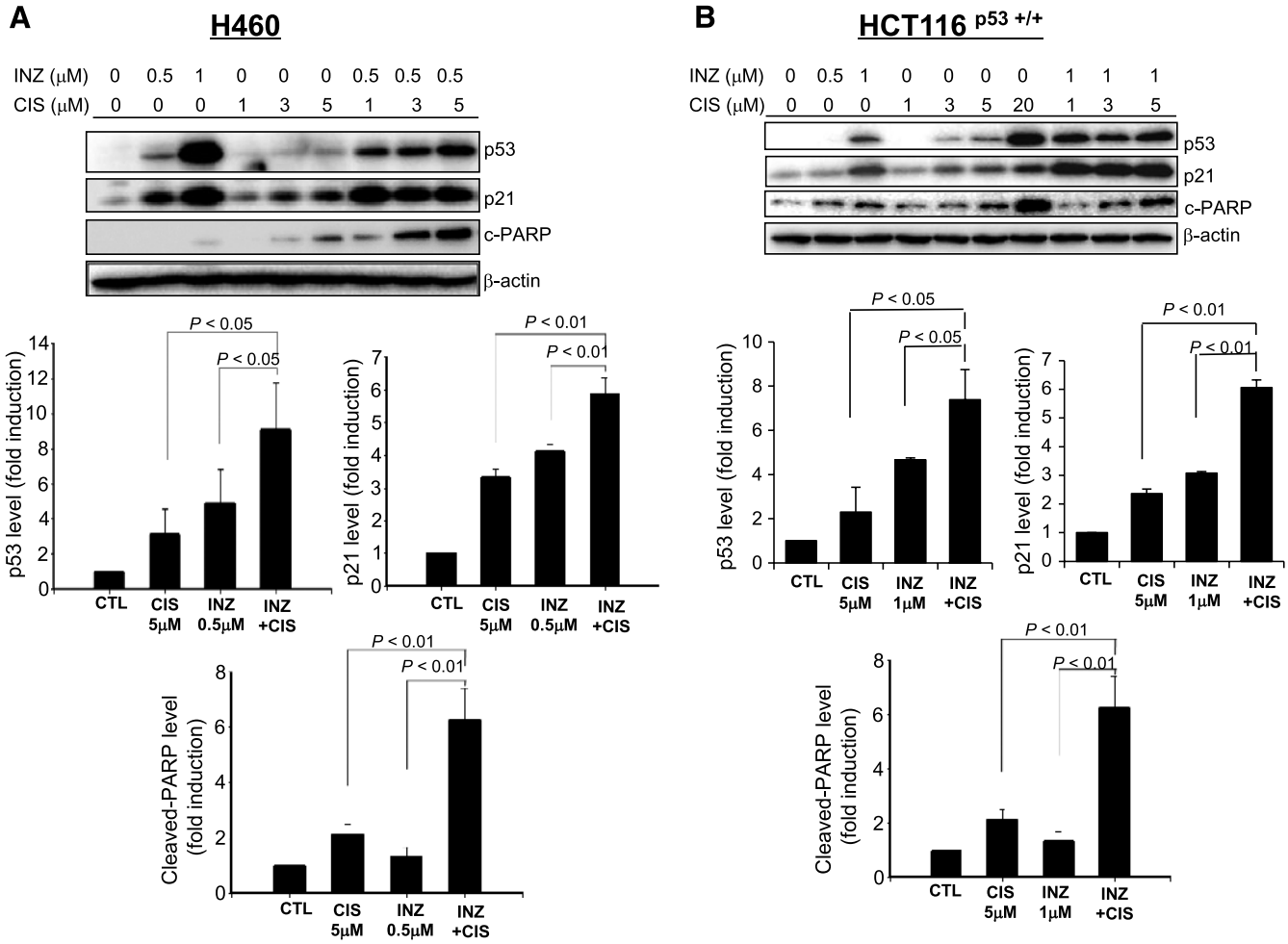

Figure 1. INZ significantly enhances CIS-induced p53 level and activity in H460 and HCT116 cells. H460 (A) or HCT116$^{p53+/+}$ (B) cells were treated with INZ or/and CIS at the indicated concentrations for 18 hours and harvested for WB analysis. Fifty micrograms of proteins was loaded to each lane, and an anti–β-actin antibody was used as a loading control. Densitometric analyses of immunoreactive bands of p53, p21, and cleaved PARP were expressed as fold change relative to the control group from at least three independent experiments (n = 3).

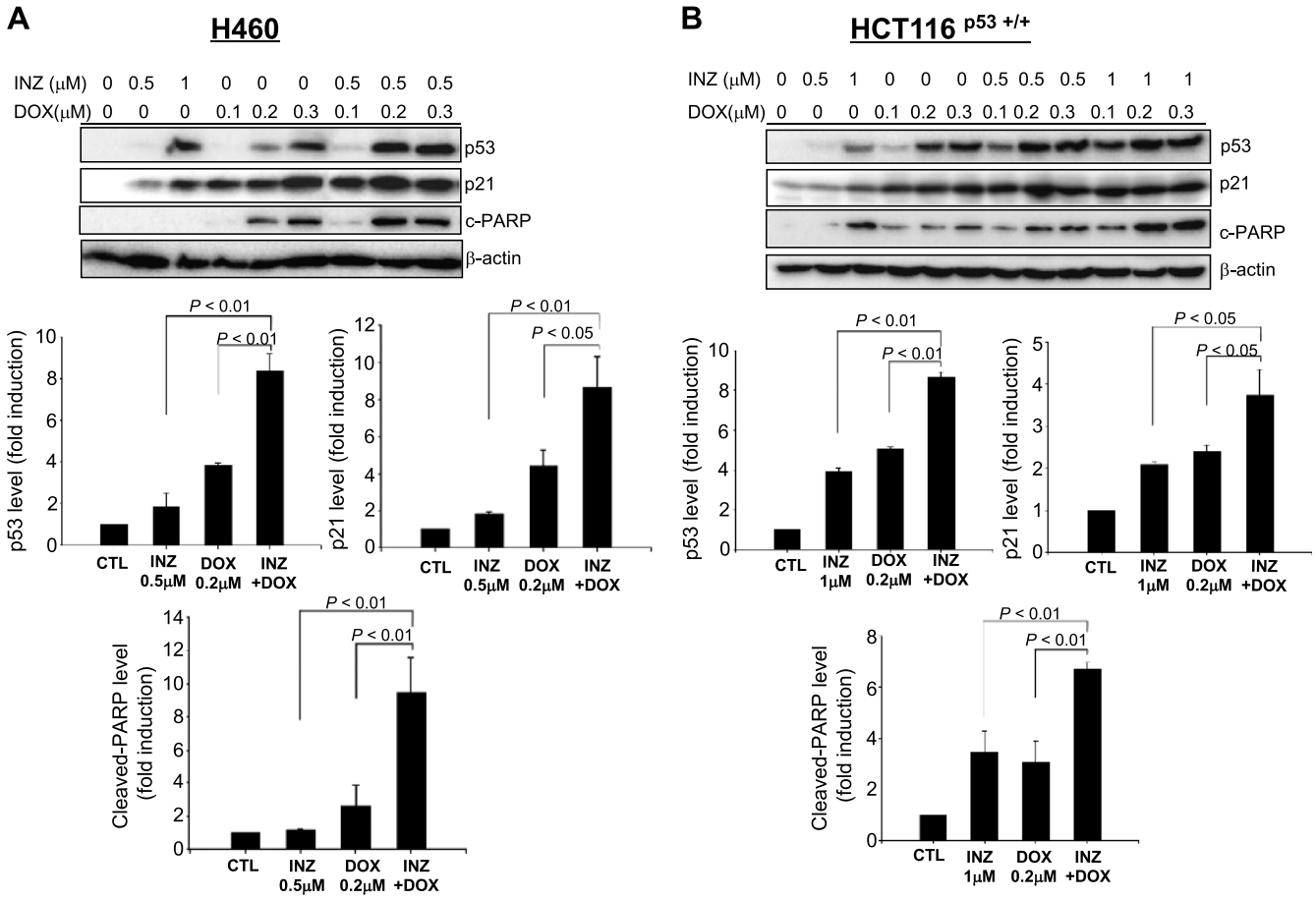

Figure 2. INZ significantly enhances DOX-induced p53 level and activity in H460 and HCT116 cells. H460 (A) or HCT116$^{p53+/+}$ (B) cells were treated with INZ or/and DOX at the indicated concentrations for 18 hours and harvested for WB analysis. Fifty micrograms of proteins was loaded to each lane, and an anti–β-actin antibody was used as a loading control. Densitometric analyses of immunoreactive bands of p53, p21, and cleaved PARP were expressed as fold change relative to the control group from three independent experiments.

Mice were subcutaneously inoculated with 2×10^6 H460 cells in the right flank, and tumor growth was monitored with calipers. After the tumors became palpable, tumor-bearing mice were randomly divided into four groups and intraperitoneally (i.p.) administered INZ (dissolved in 4% DMSO, 20 mg/kg, i.p.) once per day for 21 days as described previously [16,44], CIS (dissolved in 1% DMSO, 3 mg/kg, i.p.) once per week for 3 weeks based on previous studies [46,47], or vehicles (4% DMSO once per day and 1% DMSO once per week). Tumor volume was measured every other day, and fractional inhibition of tumor growth was calculated on the basis of the tumor volume. Mice were sacrificed by euthanasia and tumors were harvested on the last day of treatment. Tumor weight was measured and presented in histograms.

To determine the induction of p53 and apoptotic signals *in vivo*, tumor homogenates were analyzed by WB as described above.

Cell proliferation in tumors was assessed by BrdU labeling and immunofluorescence; 200 mg/kg body weight of BrdU was administrated to mice through i.p. injection 2 hours before the mice were sacrificed. *In situ* p53 expression was detected by immunofluorescence. Apoptosis was also determined by *in situ* terminal-deoxynucleoitidyl transferase-mediated nick end labelling (TUNEL) staining, using the Fluorescein *In Situ* Cell Death Detection Kit (Roche) according to the manufacturer's instructions. Briefly, tumors were fixed in 4% paraformaldehyde overnight at 4°C, embedded in paraffin, and cut into 6-μm-thick sections. Slides were boiled in fresh 10 mM sodium citrate (pH 6.0) in a steamer for 30 minutes for antigen retrieval, cooled for 30 minutes at room temperature, and washed with PBS (PBS, 0.1% Tween 20). After blocked for 1 hour in blocking buffer (PBS containing 5% goat serum and 0.3% Triton X-100), sections were incubated overnight at 4°C in a humidity chamber with a mouse anti-BrdU monoclonal antibody or a rabbit anti-p53 polyclonal antibody (FL393) diluted 1:100 in the blocking buffer, followed by incubation with an Alexa Fluor 594–conjugated or an Alexa Fluor 488–conjugated secondary antibody for 30 minutes at room temperature. Images were obtained under a fluorescence microscope (Zeiss 200), and quantitative analysis was performed using ImageJ software, by counting the positive cells in six randomly chosen fields of view, with a minimum number of 1000 cells scored for each condition.

All animal experiments were conducted in accordance with the National Institutes of Health Guide for the Care and Use of Laboratory Animals and were approved by the Institutional Animal Care and Use Committee at Indiana University School of Medicine.

Statistics

Data were reported as means ± SEM with N being the sample size. Comparisons among groups were analyzed by using one-way analysis of variance. Probability values of $P < .05$ were considered statistically significant.

Results

INZ Enhances the Potential of CIS or DOX to Activate p53

As canonic DNA-damaging anticancer drugs, CIS and DOX have been proven to kill cancer cells through multiple pathways [48], and activation of the tumor suppressor p53 is one of their major mechanisms to induce cell apoptosis and growth suppression in the cancers harboring wild-type p53 [48,49]. We recently found that INZ induces p53 by preventing the SIRT1-mediated p53 deacetylation, further inhibiting MDM2-mediated p53 degradation [16]. To test the hypothesis that INZ may potentiate the ability of CIS and DOX to activate p53, we treated p53-positive or null human non–small cell lung carcinoma cell lines H460 and H1299 with various doses of INZ, CIS or DOX alone, or of their mixtures for 18 hours, followed by WB analyses with the cell lysates as shown in Figures 1*A*, 2*A*, and W2*A*. Consistent with previous studies [16,44], INZ, CIS, or DOX by itself induced p53 level and activity (as indicated by the level of p21 and cleaved PARP) in a dose-dependent fashion in H460 cells (Figure 1*A*). Interestingly, although either of INZ at 0.5 μM, CIS at 1, 3, and 5 μM, or DOX at 0.2 μM slightly induced p53 and its target expression, combined treatment of INZ and CIS or DOX at the same lower doses significantly induced the level of p53, p21, and cleaved PARP (Figures 1*A* and 2*A*). This cooperative effect on p53 activation was also evident and reproducible in p53-positive human colon cancer cell line HCT116 (Figures 1*B* and 2*B*) and p53-positive human non–small cell lung cancer cell A549 (Figure W1). By contrast, co-treatment of p53-null cell H1299 (Figure W2*A*) or HCT116$^{p53-/-}$ (Figure W2*B*) with the same combination of the compounds did not show any significant enhancement on the level of p21 and cleaved PARP, compared to either of the single treatment, suggesting a p53-dependent cooperation of the combination. Taken together, these results indicate that INZ can cooperate with DNA-damaging reagents to activate p53 in human cancer cells.

INZ Cooperates with CIS or DOX to Inhibit p53-Dependent Cell Growth

To translate the synergy of INZ and CIS or DOX on the p53 pathway into cytotoxic effects and to demonstrate that the co-activation of the p53 pathway is indeed required for their cooperative inhibition of cancer cell growth, we carried out a set of cell survival assays by treating either H460 or HCT116$^{p53+/+}$ cells with each compound individually or two compounds simultaneously at serial dilutions in fixed molar ratios for 72 hours, as described in Materials and Methods section as well as in Figures 3 and 4. The molar concentration of a

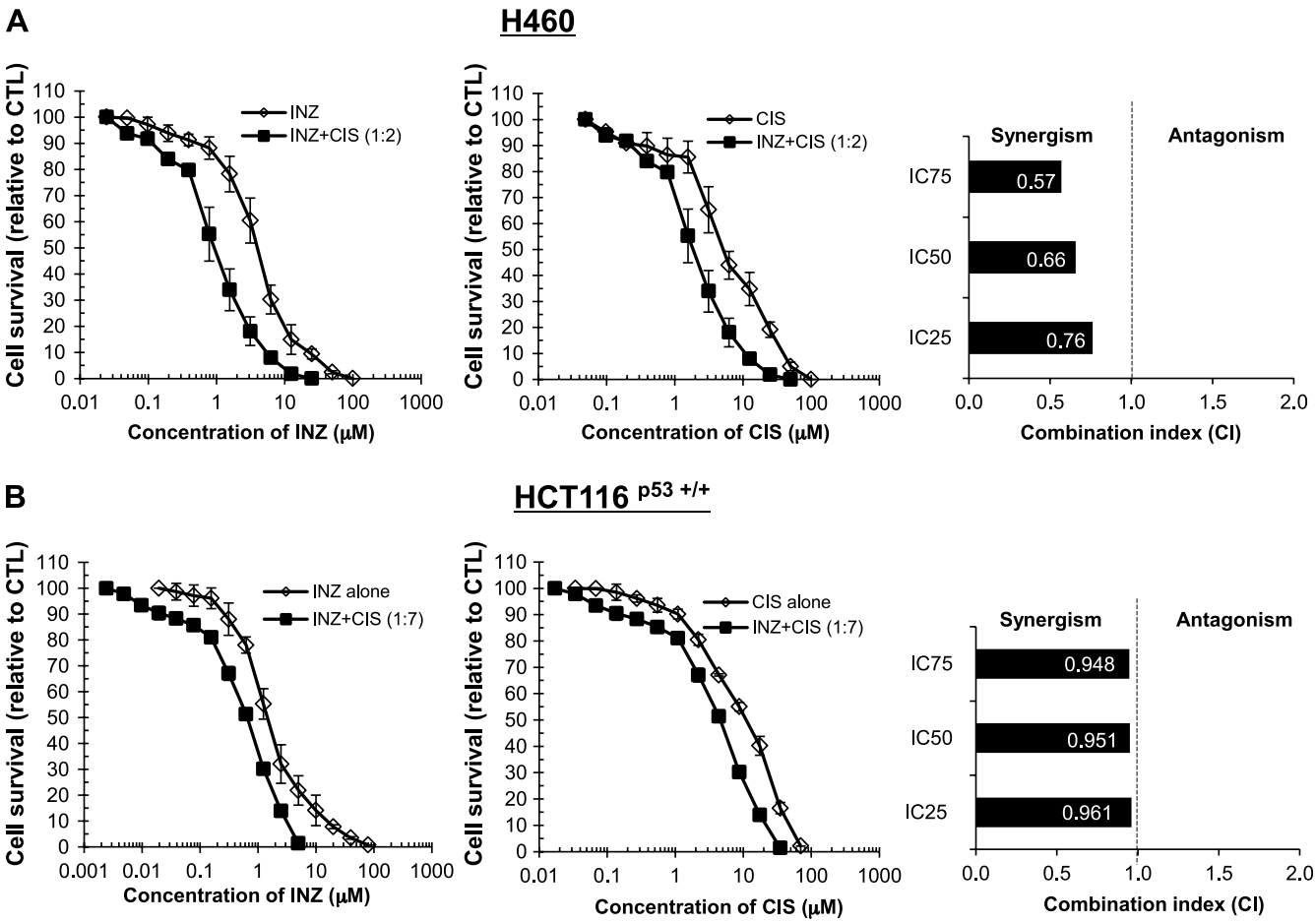

Figure 3. INZ and CIS demonstrate synergistic cytotoxicity in H460 and HCT116 cells. H460 (A) and HCT116$^{p53+/+}$ (B) cells were plated in 96-well plates and treated with INZ or CIS individually at serial dilutions or both simultaneously at fixed molar drug ratios (INZ/CIS = 1:2 for H460, INZ/CIS = 1:7 for HCT116$^{p53+/+}$) for 72 hours. Cell viability was determined using a WST cell growth assay. The data here represent the mean of three independent experiments ± SEM. CI values presented indicate the interaction of INZ with CIS when the combined treatment inhibits cell growth by 25% (IC_{25}), 50% (IC_{50}), or 75% (IC_{75}), compared to the control for their individual treatment alone.

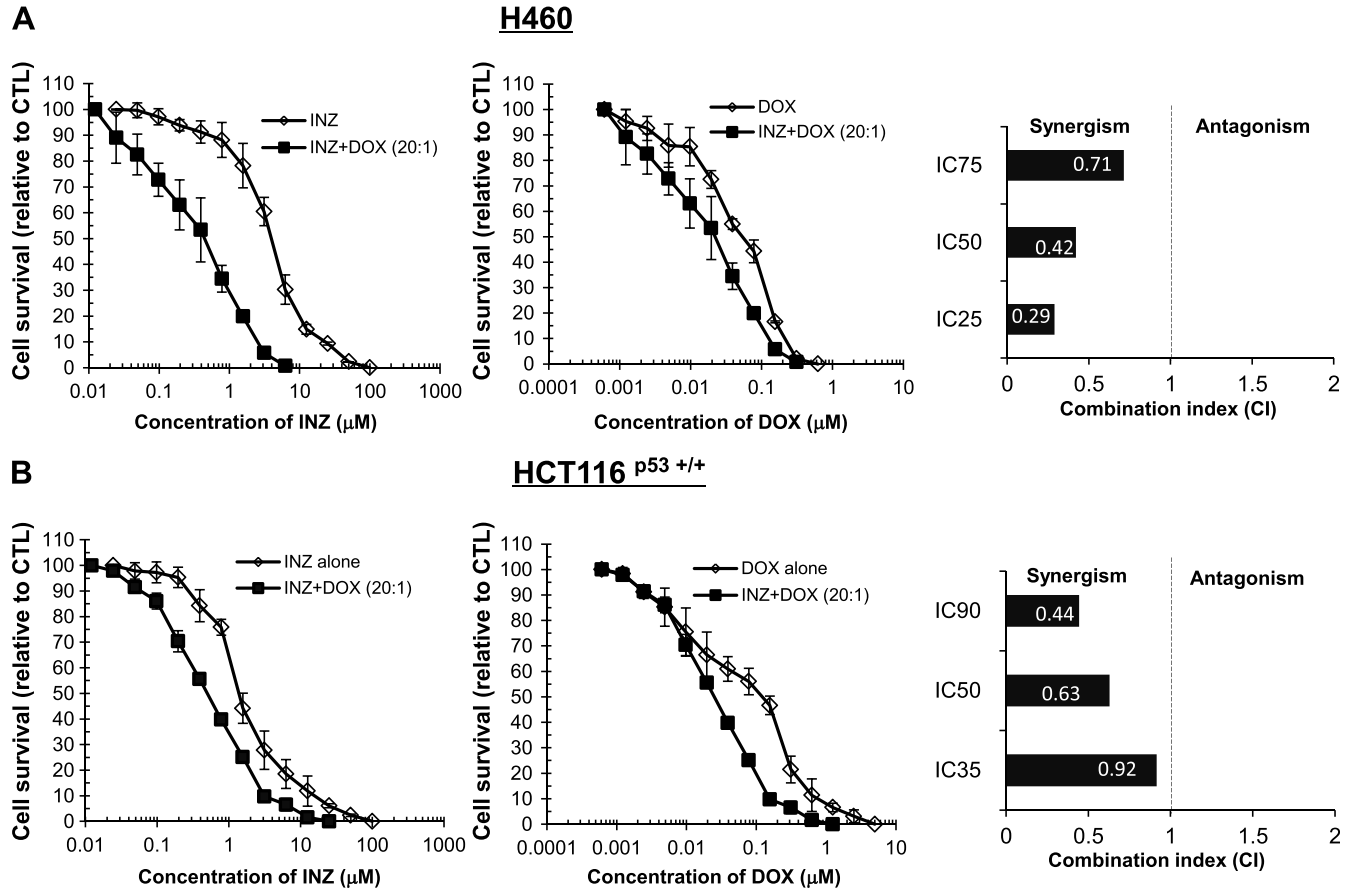

Figure 4. INZ and DOX demonstrate synergistic cytotoxicity in H460 and HCT116$^{p53+/+}$ cells. H460 (A) and HCT116$^{p53+/+}$ (B) cells were plated in 96-well plates and treated with INZ or DOX individually at serial dilutions or both simultaneously at fixed molar drug ratios (INZ/DOX = 20:1 for H460 and HCT116$^{p53+/+}$) for 72 hours. Cell viability was determined using a WST cell growth assay. The data here represent the mean of three independent experiments ± SEM. CI values presented indicate the synergy of INZ with DOX assessed as that for INZ and CIS in Figure 3.

compound required for 50% inhibition of cellular proliferation (IC_{50}) was determined for each compound to establish equipotency. The IC_{50} of INZ and CIS in H460 cells was 3 and 6 μM, respectively, indicating that the molar ratio for INZ and CIS to produce one-fold equipotency is 1:2, which was then maintained for the serial dilutions of two compounds for co-treatment (Figure 3*A*). The survival fractions of cells after single treatment or co-treatment with INZ and CIS were shown by the curves in Figure 3*A*.

The values for CI, which indicate either synergism (less than 1) or antagonism (greater than 1), were calculated as described in Materials and Methods section when the co-treatment of H460 cells with INZ and CIS reduced cellular survival by 25% (IC_{25}), 50% (IC_{50}), or 75% (IC_{75}) and plotted in the right panels of Figure 3*A*. In line with the results shown in Figure 1*A*, combination of INZ and CIS displayed obvious synergism in suppressing the growth of H460, as the CI values at a range of effective doses were clearly less than 1 (Figure 3*A*). The interplay between INZ and CIS in HCT116$^{p53+/+}$ cells (Figure 3*B*), or between INZ and DOX in H460 and HCT116$^{p53+/+}$ cells (Figure 4, *A* and *B*), was also assessed by employing the same method. As shown in Figure 4, *A* and *B*, in H460 and HCT116$^{p53+/+}$ cells, apparent synergy was evident in the co-treatment with INZ and DOX, as their CI values were obviously less than 1. The CI values for combination of INZ and CIS in HCT116$^{p53+/+}$ cells were close to but still lower than 1 (Figure 3*A*), suggesting the possible additive effect between these two compounds in this cancer cell line. However, the synergistic cell growth inhibition of INZ and CIS or DOX was not observed in p53-null cells and normal human fibroblast cell NHF-1 (Figures W2 and W3), suggesting that the synergistic suppression of cell growth by combination of INZ and CIS or DOX is p53-dependent, but not evident in normal cells. These results demonstrate that INZ and DNA-damaging drugs can synergistically repress the growth of human cancer cell lines in a p53-dependent manner.

INZ and CIS or DOX Synergistically Induce p53-Dependent Apoptosis

To further address the p53-dependent synergistic antitumor effect of INZ and DNA-damaging drugs, we detected cell apoptosis, which is one of major mechanisms for p53 to inhibit tumor growth. The results from Figures 1, 2, 3, 4, and W1 also showed the increased amount of cleaved PARP, an indicator of cell apoptosis, by co-treatment of p53-possessing H460, HCT116, and A549 cells with INZ and CIS or DOX, suggesting that this combinational treatment might induce p53-dependent apoptosis. We performed fluorescence-activated cell sorter analyses (FACS) of H460 and HCT116$^{p53+/+}$ cells after treatment with INZ and CIS or DOX for 48 hours (Figures 5 and 6). In this assay, the molar ratios of compounds for co-treatment were still maintained the same as that in the cell survival assay as described above. As shown in Figures 5*A* and 6*A*, either 2 μM CIS or 0.05 μM DOX exerted slight effects on apoptosis in H460 cells (~3% of apoptosis), whereas 1 μM INZ induced approximately 6% to 7% of apoptotic

cells. However, combinational treatment of H460 cells with the same dose of INZ and CIS (or DOX) significantly raised the apoptotic rate to 14% to 18%. For HCT116$^{p53+/+}$ cells, either 28 μM CIS or 0.2 μM DOX only induced 3% to 5% of apoptosis, and 4 μM INZ induced 6% to 7% of apoptosis; however, combined treatment dramatically increased apoptosis to ~24% and ~15%, respectively (Figures 5*B* and 6*B*). Even at lower doses of combination, additive effect was still exhibited in HCT116$^{p53+/+}$ cells (Figures 5*B* and 6*B*). Obviously, INZ sensitized these cancer cells to CIS or DOX, synergistically promoting apoptosis. This synergy on proapoptotic effect of these compounds was not seen in p53-null cells (as indicated by the level of cleaved PARP in Figure W2). Taken together, these results demonstrate that INZ and DNA-damaging drugs can synergistically suppress cell survival by inducing p53-dependent apoptosis.

INZ and CIS Cooperatively Suppress Xenograft Tumor Growth

The above results show that combination of INZ and chemotherapeutic drugs is considerably effective in suppressing the growth of wild-type p53 containing cancer cells H460 and HCT116. To translate the cooperation of these compounds into biologic significance, we further tested if INZ could also synergistically enhance the anticancer effect of CIS by employing a xenograft tumor model system derived from H460 cells. Since our previous study showed that INZ at 30 mg/kg through i.p. injection reduced the HCT116$^{p53+/+}$ tumor volume by 60% to 70% [16], or at 60 mg/kg reduced the H460 tumor volume by 50% to 60% (unpublished data), here we chose 20 mg/kg INZ for the *in vivo* study with low dose of CIS (3 mg/kg) as detailed in Materials and Methods section. As indicated in Figure 7,

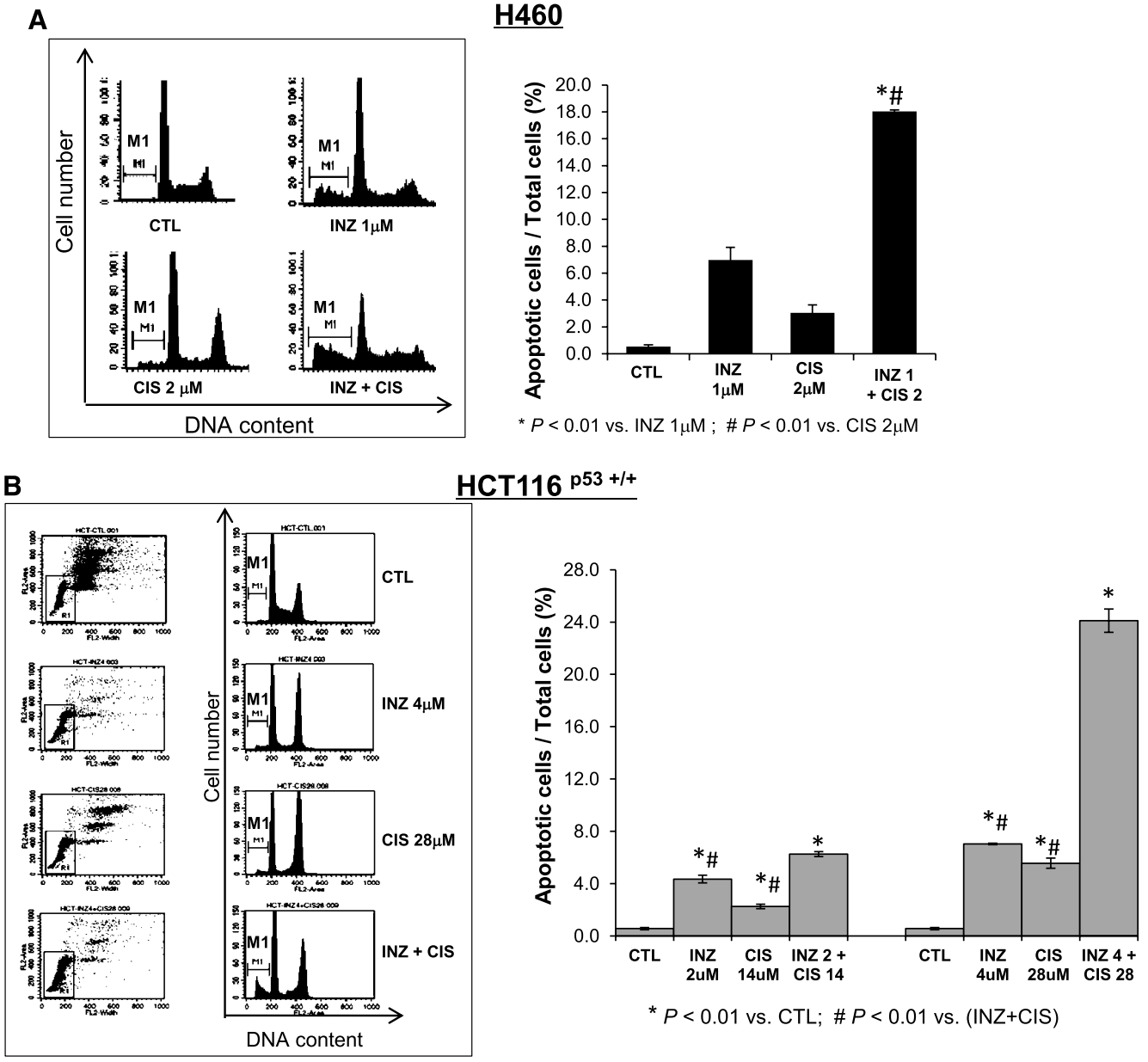

Figure 5. INZ significantly enhances the proapoptotic effect of CIS on H460 and HCT116 cells. H460 (A) and HCT116$^{p53+/+}$ (B) were plated in 6-cm-diameter dishes and treated with INZ or/and CIS at the indicated concentrations for 48 hours. Cells were stained with PI and subjected to flow cytometry to determine the DNA content. The apoptotic cells, identified by sub-G_1 DNA content, were presented as the M1 population. The data were expressed as means ± SEM (n = 4).

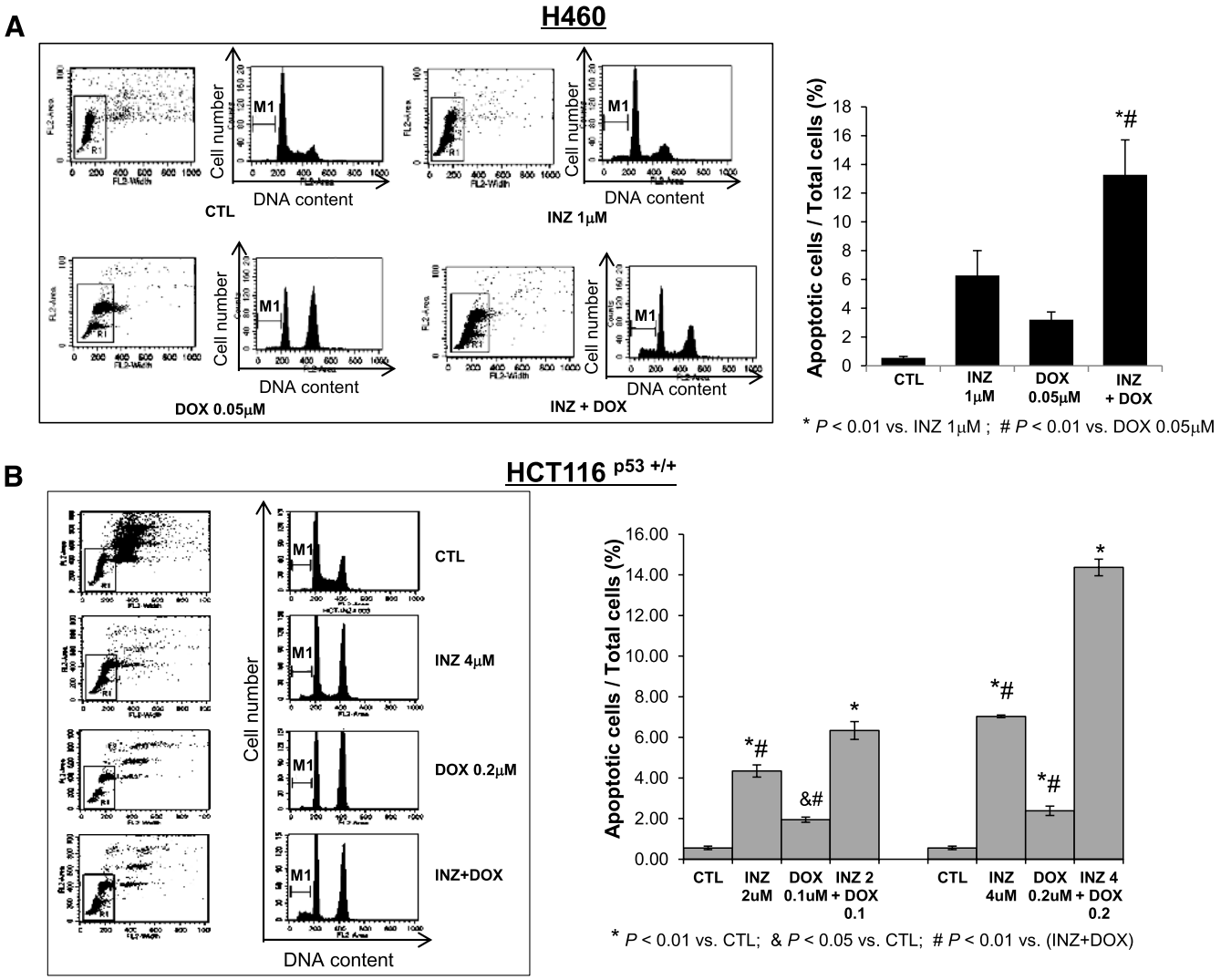

Figure 6. INZ significantly enhances the proapoptotic effect of DOX on H460 and HCT116 cells. H460 (A) and HCT116$^{p53+/+}$ (B) were plated in 6-cm-diameter dishes and treated with INZ or/and DOX at the indicated concentrations for 48 hours. Apoptotic cells were analyzed as described above in Figure 5. The data were expressed as means ± SEM (n = 4).

INZ or CIS alone reduced the average tumor volume by 25% to 30% or 45% to 50%, respectively. However, combination of the two compounds at the same doses significantly decreased the final tumor size by 80% to 85%. Furthermore, the final tumor weight also decreased to ~20% of the control by combined treatment, which displayed statistical significance compared with the other three groups (Figure 7*A*). This result confirmed that INZ could indeed potentiate CIS-induced growth suppression of H460-derived xenograft tumors *in vivo*. Consistent with this result, the two compounds synergistically induced p53 level and activity (Figure 7, *B* and *C*) as well as remarkably suppressed cell proliferation and induced apoptosis (Figure 7*C*). These results demonstrate that INZ and DNA-damaging chemotherapeutic drugs, such as CIS, can cooperatively activate p53 and suppress xenografted tumor growth in animals as well.

Discussion

Severe side effects and drug resistance are two major obstacles to limit the use of genotoxic agents, such as CIS and DOX, in systemic chemotherapy. Finding novel strategies to overcome the adverse effects and sensitize the response to existing antitumor drugs is an urgent and arduous challenge in the field of cancer chemotherapy and would have a significant clinical impact. In this study, we demonstrate that combination of INZ with low dose of CIS or DOX can synergize their abilities to significantly induce apoptosis and to inhibit growth of human wild-type p53 harboring non–small cell lung cancer cells and colon cancer cells.

Activation of the p53 pathway has been known as one of the central mechanisms for the DNA-damaging agents to induce cell apoptosis and tumor inhibition [50]. Various DNA lesions, such as CIS-caused interstrand DNA cross-linking and DOX-caused DNA double-strand breaks, trigger the activation of ATM and ATR, followed by phosphorylating downstream proteins related to cell growth, proliferation, and survival, among which p53 is the prominent protein to be phosphorylated, stabilized, and activated [51–57]. In addition, phosphorylated ChK1/2 by ATM and ATR further phosphorylates MDMX, leading to the binding between p-MDMX and 14-3-3, and results in the disruption of the interaction between MDMX and p53,

causing p53 stabilization and activation [58–61]. Maximizing the activity of p53 by concomitantly targeting different components in this pathway should be an effective approach to impede the growth of tumors harboring functional p53. INZ, as reported previously by our group, is a potent nongenotoxic p53 activator by inhibiting SIRT1-mediated deacetylation [16]. Combination of DNA-damaging agents with INZ would not only induce the phosphorylation of p53 in response to activation of ATM and ATR but also increase the acetylation and weaken the ubiquitination of p53 due to inactivated SIRT1. The sum outcome of this double treatment is, therefore, the more remarkable induction of p53 level and activity. Indeed, as expected, in both p53-containing H460 and HCT116 cells, p53 level and activity (indicated by the p21 level) exhibited a dramatic augment after combined treatment with INZ and CIS or DOX, even at relatively lower doses, compared with either of the single treatment (Figures 1, 2, and W1). Our subsequent results further proved the p53-dependent cooperation between INZ and genotoxic drugs, particularly CIS, on cell growth inhibition, which might be attributed to the augment of apoptotic response, in p53 wild-type cells but not in p53-null cells (Figures 3, 4, 5, 6, and W2).

One of the most strenuous challenges for the oncologists in current cancer chemotherapeutic practice is the cumulative and dose-dependent toxicity to normal tissues, such as nephrotoxicity and cardiomyopathy caused by CIS and DOX, respectively. Both CIS and DOX have been supposed to cause side effects by some mechanisms different from the typical DNA lesions that are primarily responsible for their suppression on tumor growth [3,5,62,63]. For instance, CIS may be metabolized to a reactive toxic thiol by some enzymes such as γ-glutamyl transpeptidase whose high level in renal proximal tubular cells sensitizes the cells to CIS toxicity and further target the mitochondria and endoplasmic reticulum of the proximal tubular cells [5,64–66]. Several approaches have been developed against the toxicity, including application of prodrugs and derivatives [67,68], combination with some specific protectors such as antioxidants [69–71], and improvement of drug delivery systems [72–74]. Lowering drug dosage by combination with agents with different mechanisms of action should be a simple, feasible, and effective means to minimize the side effects of DNA-interfering drugs, while retaining the antitumor effects. Again, our results prove that INZ possesses this kind of capability based on its specific p53 induction

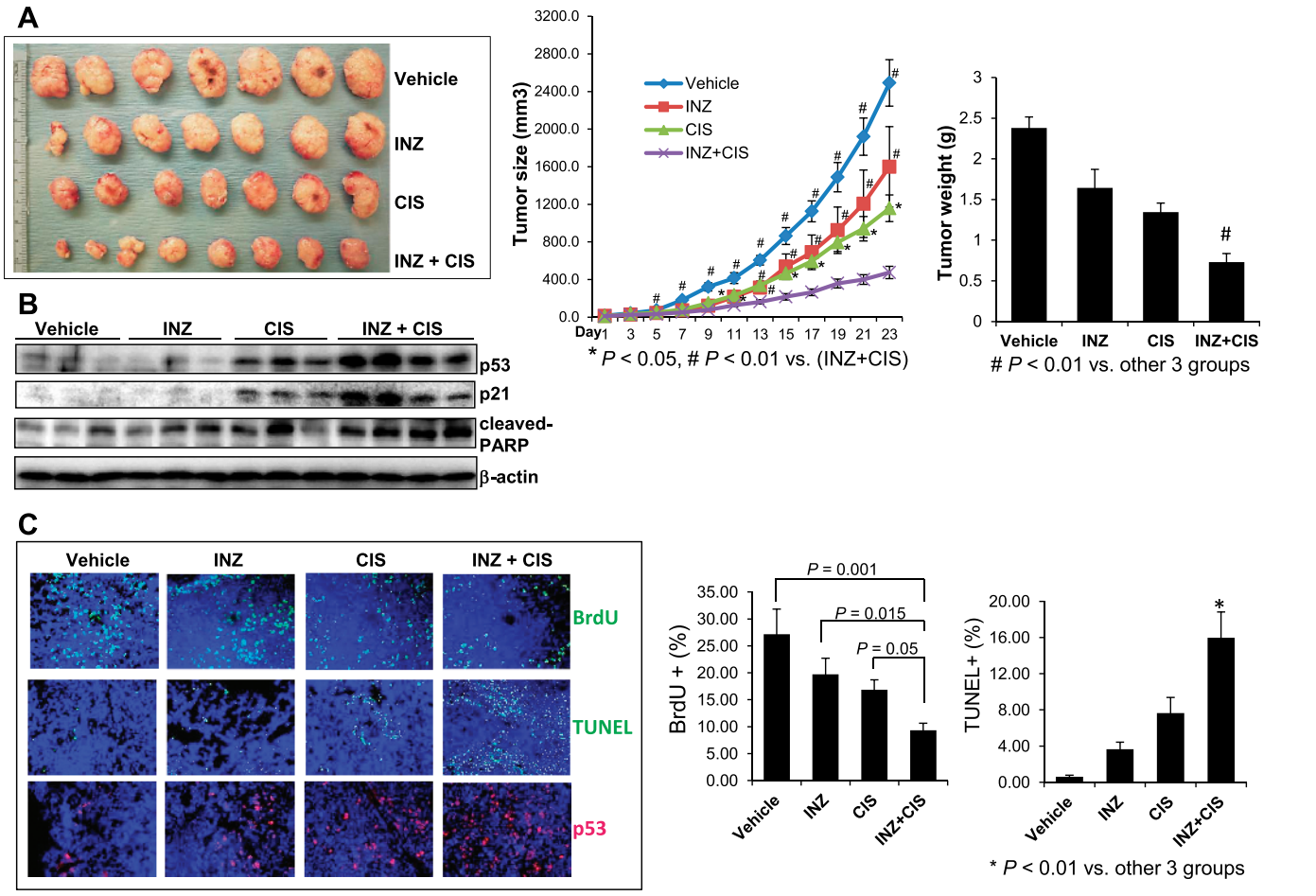

Figure 7. INZ significantly enhances CIS-induced p53 activation, apoptosis, and tumor suppression. (A) Combination of INZ and CIS markedly suppresses the growth of xenograft tumors derived from H460 cells. Mice bearing H460 xenografts were i.p. treated with INZ (20 mg/kg) everyday or/and CIS (3 mg/kg) once per week or vehicles for 21 days. Images of tumors isolated are presented at the left. The tumor growth is shown by the mean tumor volumes ± SEM (middle), and the final tumor weight is shown in columns (right; $n = 6$ mice per group; $^*P < .05$). (B) WB analysis of proteins extracted from H460 tumor samples in A with antibodies as indicated on the right. (C) Representative images of TUNEL staining, BrdU, and p53 immunostaining of xenograft tumor sections are presented. Quantification of BrdU and TUNEL staining is expressed as mean ± SEM ($n = 4$ mice per group).

in tumors and minimal side effects on normal cells and tissues [16], as even much lower doses of CIS or INZ are required for combined therapy to achieve a satisfactory anticancer effect on tumor xenografts with wild-type p53 (Figure 7), but the same combination exerted little synergistic effect on normal cells (Figure W3). Even though more studies are needed to further illuminate the low toxicity of INZ in normal cells and tissues, INZ could be a promising component for adjuvant antitumor therapy.

Another major cause of treatment failure during tumor chemotherapy is drug resistance, which is a complicated multifactorial event. Taking CIS as an example again, the chemoresistance may involve many aspects, including loss of apoptotic response [41,75], overactivation of survival signals such as phosphatidylinositol 3-kinase (PI3K)/Akt [40,42,76–78], increased DNA repair [79–82], induction of multidrug resistance [83,84], increased efflux, and decreased influx of the drug [82]. A number of *in vitro*, *in vivo*, and clinical studies support p53 as an important regulator during most of these processes to mediate the drug sensitivity [40–42,75,76,85–95]. Activation of prosurvival factor Akt [40,76], CBP/p300-interacting transactivator protein CITED2 [96], which is critical for cell growth and oncogenesis [96], oncogenic phosphatase protein PPM1D [41], or protein trafficking related protein NAPA [90] renders cancer cells resistant to chemotherapy, while suppression of their activity sensitizes cells to CIS, which requires the activation of wild-type p53. P53-HDAC2 complex represses the expression of multidrug resistance–related protein lung resistance–related protein (LRP) through binding to the LRP promoter, whereas loss of p53-mediated suppression on LRP may cause the chemoresistance in tumor cells [86]. Down-regulation of p53 in human breast cancer cells increases the CIS resistance mediated by variant, which is one of the factors in charge of DNA repair and telomere maintenance [97]. Restoration or reactivation of wild-type p53 dramatically improved the apoptotic response and sensitivity to CIS in tumor cells [49,85,98–100]. On the basis of these findings, it would be rational to sensitize the chemotherapy by specifically targeting p53, with very low possibility to induce a secondary pathway related to drug resistance. Our study as presented here indeed demonstrates that the specific p53 inducer INZ can sensitize cancer cells, particularly the lung cancer cell line H460 whose chemotherapy is mainly composed of CIS-based regimen, to low dose of CIS, leading to tumor suppression in a p53-dependent manner (Figures 3–7 and W2). Studies on chemoresistant cancer cell lines are necessary to further address the beneficial effects of combination with INZ and chemotherapy on drug sensitivity. Nevertheless, taken together, our current findings suggest that specifically targeting the p53 pathway promotes the sensitivity of cancer cells to traditional chemotherapeutic drugs, and combination of INZ with standard chemotherapy will provide an attractive anticancer protocol for the cancer patients with high sensitivity to side effects and refractory drug resistance in the future.

Acknowledgments

We thank the members of the Lu Laboratory for active discussion.

References

[1] Dy GK and Adjei AA (2008). Systemic cancer therapy: evolution over the last 60 years. *Cancer* **113**, 1857–1887.

[2] Boulikas T and Vougiouka M (2003). Cisplatin and platinum drugs at the molecular level (Review). *Oncol Rep* **10**, 1663–1682.

[3] Wallace KB (2003). Doxorubicin-induced cardiac mitochondrionopathy. *Pharmacol Toxicol* **93**, 105–115.

[4] Gonzales-Vitale JC, Hayes DM, Cvitkovic E, and Sternberg SS (1977). The renal pathology in clinical trials of cis-platinum (II) diamminedichloride. *Cancer* **39**, 1362–1371.

[5] Hanigan MH and Devarajan P (2003). Cisplatin nephrotoxicity: molecular mechanisms. *Cancer Ther* **1**, 47–61.

[6] Lipshultz SE, Colan SD, Gelber RD, Perez-Atayde AR, Sallan SE, and Sanders SP (1991). Late cardiac effects of doxorubicin therapy for acute lymphoblastic leukemia in childhood. *N Engl J Med* **324**, 808–815.

[7] Zhang YW, Shi J, Li YJ, and Wei L (2009). Cardiomyocyte death in doxorubicin-induced cardiotoxicity. *Arch Immunol Ther Exp (Warsz)* **57**, 435–445.

[8] Singal PK and Iliskovic N (1998). Doxorubicin-induced cardiomyopathy. *N Engl J Med* **339**, 900–905.

[9] Baird RD and Kaye SB (2003). Drug resistance reversal—are we getting closer? *Eur J Cancer* **39**, 2450–2461.

[10] Lane D and Levine A (2010). p53 Research: the past thirty years and the next thirty years. *Cold Spring Harb Perspect Biol* **2**, a000893.

[11] Leung AK and Sharp PA (2010). MicroRNA functions in stress responses. *Mol Cell* **40**, 205–215.

[12] Boominathan L (2010). The guardians of the genome (p53, TA-p73, and TA-p63) are regulators of tumor suppressor miRNAs network. *Cancer Metastasis Rev* **29**, 613–639.

[13] Hollstein M, Sidransky D, Vogelstein B, and Harris CC (1991). p53 Mutations in human cancers. *Science* **253**, 49–53.

[14] Vogelstein B, Lane D, and Levine AJ (2000). Surfing the p53 network. *Nature* **408**, 307–310.

[15] Petitjean A, Mathe E, Kato S, Ishioka C, Tavtigian SV, Hainaut P, and Olivier M (2007). Impact of mutant p53 functional properties on TP53 mutation patterns and tumor phenotype: lessons from recent developments in the IARC TP53 database. *Hum Mutat* **28**, 622–629.

[16] Zhang Q, Zeng SX, Zhang Y, Zhang Y, Ding D, Ye Q, Meroueh SO, and Lu H (2012). A small molecule Inauhzin inhibits SIRT1 activity and suppresses tumour growth through activation of p53. *EMBO Mol Med* **4**, 298–312.

[17] Momand J, Zambetti GP, Olson DC, George D, and Levine AJ (1992). The *mdm-2* oncogene product forms a complex with the p53 protein and inhibits p53-mediated transactivation. *Cell* **69**, 1237–1245.

[18] Oliner JD, Pietenpol JA, Thiagalingam S, Gyuris J, Kinzler KW, and Vogelstein B (1993). Oncoprotein MDM2 conceals the activation domain of tumour suppressor p53. *Nature* **362**, 857–860.

[19] Kruse JP and Gu W (2009). Modes of p53 regulation. *Cell* **137**, 609–622.

[20] Wade M, Wang YV, and Wahl GM (2010). The p53 orchestra: Mdm2 and Mdmx set the tone. *Trends Cell Biol* **20**, 299–309.

[21] Kawai H, Lopez-Pajares V, Kim MM, Wiederschain D, and Yuan ZM (2007). RING domain–mediated interaction is a requirement for MDM2's E3 ligase activity. *Cancer Res* **67**, 6026–6030.

[22] Linke K, Mace PD, Smith CA, Vaux DL, Silke J, and Day CL (2008). Structure of the MDM2/MDMX RING domain heterodimer reveals dimerization is required for their ubiquitylation in trans. *Cell Death Differ* **15**, 841–848.

[23] Wu X, Bayle JH, Olson D, and Levine AJ (1993). The p53-mdm-2 autoregulatory feedback loop. *Genes Dev* **7**, 1126–1132.

[24] Levine AJ and Oren M (2009). The first 30 years of p53: growing ever more complex. *Nat Rev Cancer* **9**, 749–758.

[25] Shangary S and Wang S (2009). Small-molecule inhibitors of the MDM2-p53 protein-protein interaction to reactivate p53 function: a novel approach for cancer therapy. *Annu Rev Pharmacol Toxicol* **49**, 223–241.

[26] Vassilev LT, Vu BT, Graves B, Carvajal D, Podlaski F, Filipovic Z, Kong N, Kammlott U, Lukacs C, Klein C, et al. (2004). *In vivo* activation of the p53 pathway by small-molecule antagonists of MDM2. *Science* **303**, 844–848.

[27] Issaeva N, Bozko P, Enge M, Protopopova M, Verhoef LG, Masucci M, Pramanik A, and Selivanova G (2004). Small molecule RITA binds to p53, blocks p53-HDM-2 interaction and activates p53 function in tumors. *Nat Med* **10**, 1321–1328.

[28] Shangary S, Qin D, McEachern D, Liu M, Miller RS, Qiu S, Nikolovska-Coleska Z, Ding K, Wang G, Chen J, et al. (2008). Temporal activation of p53 by a specific MDM2 inhibitor is selectively toxic to tumors and leads to complete tumor growth inhibition. *Proc Natl Acad Sci USA* **105**, 3933–3938.

[29] Yang Y, Ludwig RL, Jensen JP, Pierre SA, Medaglia MV, Davydov IV, Safiran YJ, Oberoi P, Kenten JH, Phillips AC, et al. (2005). Small molecule inhibitors of HDM2 ubiquitin ligase activity stabilize and activate p53 in cells. *Cancer Cell* **7**, 547–559.

[30] Reed D, Shen Y, Shelat AA, Arnold LA, Ferreira AM, Zhu F, Mills N, Smithson DC, Regni CA, Bashford D, et al. (2010). Identification and characterization of the first small molecule inhibitor of MDMX. *J Biol Chem* **285**, 10786–10796.

[31] Kobet E, Zeng X, Zhu Y, Keller D, and Lu H (2000). MDM2 inhibits p300-mediated p53 acetylation and activation by forming a ternary complex with the two proteins. *Proc Natl Acad Sci USA* **97**, 12547–12552.

[32] Ito A, Lai CH, Zhao X, Saito S, Hamilton MH, Appella E, and Yao TP (2001). p300/CBP-mediated p53 acetylation is commonly induced by p53-activating agents and inhibited by MDM2. *EMBO J* **20**, 1331–1340.

[33] Gu W and Roeder RG (1997). Activation of p53 sequence-specific DNA binding by acetylation of the p53 C-terminal domain. *Cell* **90**, 595–606.

[34] Li M, Luo J, Brooks CL, and Gu W (2002). Acetylation of p53 inhibits its ubiquitination by Mdm2. *J Biol Chem* **277**, 50607–50611.

[35] Ito A, Kawaguchi Y, Lai CH, Kovacs JJ, Higashimoto Y, Appella E, and Yao TP (2002). MDM2-HDAC1-mediated deacetylation of p53 is required for its degradation. *EMBO J* **21**, 6236–6245.

[36] Huffman DM, Grizzle WE, Bamman MM, Kim JS, Eltoum IA, Elgavish A, and Nagy TR (2007). SIRT1 is significantly elevated in mouse and human prostate cancer. *Cancer Res* **67**, 6612–6618.

[37] Jung-Hynes B, Nihal M, Zhong W, and Ahmad N (2009). Role of sirtuin histone deacetylase SIRT1 in prostate cancer. A target for prostate cancer management via its inhibition? *J Biol Chem* **284**, 3823–3832.

[38] Chen WY, Wang DH, Yen RC, Luo J, Gu W, and Baylin SB (2005). Tumor suppressor HIC1 directly regulates SIRT1 to modulate p53-dependent DNA-damage responses. *Cell* **123**, 437–448.

[39] Lain S, Hollick JJ, Campbell J, Staples OD, Higgins M, Aoubala M, McCarthy A, Appleyard V, Murray KE, Baker L, et al. (2008). Discovery, *in vivo* activity, and mechanism of action of a small-molecule p53 activator. *Cancer Cell* **13**, 454–463.

[40] Fraser M, Bai T, and Tsang BK (2008). Akt promotes cisplatin resistance in human ovarian cancer cells through inhibition of p53 phosphorylation and nuclear function. *Int J Cancer* **122**, 534–546.

[41] Ali AY, Abedini MR, and Tsang BK (2012). The oncogenic phosphatase PPM1D confers cisplatin resistance in ovarian carcinoma cells by attenuating checkpoint kinase 1 and p53 activation. *Oncogene* **31**, 2175–2186.

[42] Fraser M, Leung BM, Yan X, Dan HC, Cheng JQ, and Tsang BK (2003). p53 is a determinant of X-linked inhibitor of apoptosis protein/Akt-mediated chemoresistance in human ovarian cancer cells. *Cancer Res* **63**, 7081–7088.

[43] Song K, Cowan KH, and Sinha BK (1999). *In vivo* studies of adenovirus-mediated p53 gene therapy for cis-platinum-resistant human ovarian tumor xenografts. *Oncol Res* **11**, 153–159.

[44] Zhang Y, Zhang Q, Zeng SX, Mayo LD, and Lu H (2012). Inauhzin and Nutlin3 synergistically activate p53 and suppress tumor growth. *Cancer Biol Ther* **13**, 915–924.

[45] Chou TC and Talalay P (1984). Quantitative analysis of dose-effect relationships: the combined effects of multiple drugs or enzyme inhibitors. *Adv Enzyme Regul* **22**, 27–55.

[46] Jafri SH, Glass J, Shi R, Zhang S, Prince M, and Kleiner-Hancock H (2010). Thymoquinone and cisplatin as a therapeutic combination in lung cancer: *in vitro* and *in vivo*. *J Exp Clin Cancer Res* **29**, 87.

[47] Carter CA, Chen C, Brink C, Vincent P, Maxuitenko YY, Gilbert KS, Waud WR, and Zhang X (2007). Sorafenib is efficacious and tolerated in combination with cytotoxic or cytostatic agents in preclinical models of human non-small cell lung carcinoma. *Cancer Chemother Pharmacol* **59**, 183–195.

[48] Siddik ZH (2003). Cisplatin: mode of cytotoxic action and molecular basis of resistance. *Oncogene* **22**, 7265–7279.

[49] Gutekunst M, Oren M, Weilbacher A, Dengler MA, Markwardt C, Thomale J, Aulitzky WE, and van der Kuip H (2011). p53 hypersensitivity is the predominant mechanism of the unique responsiveness of testicular germ cell tumor (TGCT) cells to cisplatin. *PLoS One* **6**, e19198.

[50] Johnstone RW, Ruefli AA, and Lowe SW (2002). Apoptosis: a link between cancer genetics and chemotherapy. *Cell* **108**, 153–164.

[51] Harper JW and Elledge SJ (2007). The DNA damage response: ten years after. *Mol Cell* **28**, 739–745.

[52] Bartek J, Bartkova J, and Lukas J (2007). DNA damage signalling guards against activated oncogenes and tumour progression. *Oncogene* **26**, 7773–7779.

[53] Zhou BB and Elledge SJ (2000). The DNA damage response: putting checkpoints in perspective. *Nature* **408**, 433–439.

[54] Jackson SP and Bartek J (2009). The DNA-damage response in human biology and disease. *Nature* **461**, 1071–1078.

[55] Sancar A, Lindsey-Boltz LA, Unsal-Kacmaz K, and Linn S (2004). Molecular mechanisms of mammalian DNA repair and the DNA damage checkpoints. *Annu Rev Biochem* **73**, 39–85.

[56] Hurley PJ and Bunz F (2007). ATM and ATR: components of an integrated circuit. *Cell Cycle* **6**, 414–417.

[57] Cimprich KA and Cortez D (2008). ATR: an essential regulator of genome integrity. *Nat Rev Mol Cell Biol* **9**, 616–627.

[58] Lee JH, Jin Y, He G, Zeng SX, Wang YV, Wahl GM, and Lu H (2012). Hypoxia activates tumor suppressor p53 by inducing ATR-Chk1 kinase cascade-mediated phosphorylation and consequent 14-3-3γ inactivation of MDMX protein. *J Biol Chem* **287**, 20898–20903.

[59] Jin Y, Dai MS, Lu SZ, Xu Y, Luo Z, Zhao Y, and Lu H (2006). 14-3-3γ binds to MDMX that is phosphorylated by UV-activated Chk1, resulting in p53 activation. *EMBO J* **25**, 1207–1218.

[60] LeBron C, Chen L, Gilkes DM, and Chen J (2006). Regulation of MDMX nuclear import and degradation by Chk2 and 14-3-3. *EMBO J* **25**, 1196–1206.

[61] Chen L, Gilkes DM, Pan Y, Lane WS, and Chen J (2005). ATM and Chk2-dependent phosphorylation of MDMX contribute to p53 activation after DNA damage. *EMBO J* **24**, 3411–3422.

[62] Iarussi D, Indolfi P, Casale F, Coppolino P, Tedesco MA, and Di Tullio MT (2001). Recent advances in the prevention of anthracycline cardiotoxicity in childhood. *Curr Med Chem* **8**, 1649–1660.

[63] Neilan TG, Blake SL, Ichinose F, Raher MJ, Buys ES, Jassal DS, Furutani E, Perez-Sanz TM, Graveline A, Janssens SP, et al. (2007). Disruption of nitric oxide synthase 3 protects against the cardiac injury, dysfunction, and mortality induced by doxorubicin. *Circulation* **116**, 506–514.

[64] Hanigan MH, Gallagher BC, Townsend DM, and Gabarra V (1999). γ-Glutamyl transpeptidase accelerates tumor growth and increases the resistance of tumors to cisplatin *in vivo*. *Carcinogenesis* **20**, 553–559.

[65] Hanigan MH, Lykissa ED, Townsend DM, Ou CN, Barrios R, and Lieberman MW (2001). γ-glutamyl transpeptidase-deficient mice are resistant to the nephrotoxic effects of cisplatin. *Am J Pathol* **159**, 1889–1894.

[66] Wainford RD, Weaver RJ, Stewart KN, Brown P, and Hawksworth GM (2008). Cisplatin nephrotoxicity is mediated by gamma glutamyltranspeptidase, not via a C-S lyase governed biotransformation pathway. *Toxicology* **249**, 184–193.

[67] Dhar S, Kolishetti N, Lippard SJ, and Farokhzad OC (2011). Targeted delivery of a cisplatin prodrug for safer and more effective prostate cancer therapy *in vivo*. *Proc Natl Acad Sci USA* **108**, 1850–1855.

[68] Lebrecht D, Geist A, Ketelsen UP, Haberstroh J, Setzer B, Kratz F, and Walker UA (2007). The 6-maleimidocaproyl hydrazone derivative of doxorubicin (DOXO-EMCH) is superior to free doxorubicin with respect to cardiotoxicity and mitochondrial damage. *Int J Cancer* **120**, 927–934.

[69] Lebrecht D, Geist A, Ketelsen UP, Haberstroh J, Setzer B, and Walker UA (2007). Dexrazoxane prevents doxorubicin-induced long-term cardiotoxicity and protects myocardial mitochondria from genetic and functional lesions in rats. *Br J Pharmacol* **151**, 771–778.

[70] Hensley ML, Hagerty KL, Kewalramani T, Green DM, Meropol NJ, Wasserman TH, Cohen GI, Emami B, Gradishar WJ, Mitchell RB, et al. (2009). American Society of Clinical Oncology 2008 clinical practice guideline update: use of chemotherapy and radiation therapy protectants. *J Clin Oncol* **27**, 127–145.

[71] Asna N, Lewy H, Ashkenazi IE, Deutsch V, Peretz H, Inbar M, and Ron IG (2005). Time dependent protection of amifostine from renal and hematopoietic cisplatin induced toxicity. *Life Sci* **76**, 1825–1834.

[72] Kuang Y, Liu J, Liu Z, and Zhuo R (2012). Cholesterol-based anionic long-circulating cisplatin liposomes with reduced renal toxicity. *Biomaterials* **33**, 1596–1606.

[73] Rigacci L, Mappa S, Nassi L, Alterini R, Carrai V, Bernardi F, and Bosi A (2007). Liposome-encapsulated doxorubicin in combination with cyclophosphamide, vincristine, prednisone and rituximab in patients with lymphoma and concurrent cardiac diseases or pre-treated with anthracyclines. *Hematol Oncol* **25**, 198–203.

[74] Yildirim Y, Gultekin E, Avci ME, Inal MM, Yunus S, and Tinar S (2008). Cardiac safety profile of pegylated liposomal doxorubicin reaching or exceeding lifetime cumulative doses of 550 mg/m2 in patients with recurrent ovarian and peritoneal cancer. *Int J Gynecol Cancer* **18**, 223–227.

[75] Sato S, Kigawa J, Minagawa Y, Okada M, Shimada M, Takahashi M, Kamazawa S, and Terakawa N (1999). Chemosensitivity and p53-dependent apoptosis in epithelial ovarian carcinoma. *Cancer* **86**, 1307–1313.

[76] Yang X, Fraser M, Moll UM, Basak A, and Tsang BK (2006). Akt-mediated cisplatin resistance in ovarian cancer: modulation of p53 action on caspase-dependent mitochondrial death pathway. *Cancer Res* **66**, 3126–3136.

[77] Lee S, Choi EJ, Jin C, and Kim DH (2005). Activation of PI3K/Akt pathway by PTEN reduction and PIK3CA mRNA amplification contributes to cisplatin resistance in an ovarian cancer cell line. *Gynecol Oncol* **97**, 26–34.

[78] Riedel RF, Porrello A, Pontzer E, Chenette EJ, Hsu DS, Balakumaran B, Potti A, Nevins J, and Febbo PG (2008). A genomic approach to identify molecular pathways associated with chemotherapy resistance. *Mol Cancer Ther* **7**, 3141–3149.

[79] Barakat K, Gajewski M, and Tuszynski JA (2012). DNA repair inhibitors: the next major step to improve cancer therapy. *Curr Top Med Chem* **12**, 1376–1390.

[80] Pan Y, Zhang Q, Atsaves V, Yang H, and Claret FX (2012). Suppression of Jab1/CSN5 induces radio- and chemo-sensitivity in nasopharyngeal carcinoma through changes to the DNA damage and repair pathways. *Oncogene*, 1–11. doi: 10.1038/onc2012.294.

[81] Wilk A, Waligorska A, Waligorski P, Ochoa A, and Reiss K (2012). Inhibition of ERβ induces resistance to cisplatin by enhancing Rad51-mediated DNA repair in human medulloblastoma cell lines. *PLoS One* **7**, e33867.

[82] Chu G (1994). Cellular responses to cisplatin. The roles of DNA-binding proteins and DNA repair. *J Biol Chem* **269**, 787–790.

[83] Itoh Y, Tamai M, Yokogawa K, Nomura M, Moritani S, Suzuki H, Sugiyama Y, and Miyamoto K (2002). Involvement of multidrug resistance-associated protein 2 in *in vivo* cisplatin resistance of rat hepatoma AH66 cells. *Anticancer Res* **22**, 1649–1653.

[84] To KK, Yu L, Liu S, Fu J, and Cho CH (2012). Constitutive AhR activation leads to concomitant ABCG2-mediated multidrug resistance in cisplatin-resistant esophageal carcinoma cells. *Mol Carcinog* **51**, 449–464.

[85] Guntur VP, Waldrep JC, Guo JJ, Selting K, and Dhand R (2010). Increasing p53 protein sensitizes non-small cell lung cancer to paclitaxel and cisplatin *in vitro*. *Anticancer Res* **30**, 3557–3564.

[86] Tian B, Liu J, Liu B, Dong Y, Song Y, and Sun Z (2011). p53 Suppresses lung resistance-related protein expression through Y-box binding protein 1 in the MCF-7 breast tumor cell line. *J Cell Physiol* **226**, 3433–3441.

[87] Han JY, Lee GK, Jang DH, Lee SY, and Lee JS (2008). Association of p53 codon 72 polymorphism and MDM2 SNP309 with clinical outcome of advanced nonsmall cell lung cancer. *Cancer* **113**, 799–807.

[88] Ikuta K, Takemura K, Kihara M, Naito S, Lee E, Shimizu E, and Yamauchi A (2005). Defects in apoptotic signal transduction in cisplatin-resistant non-small cell lung cancer cells. *Oncol Rep* **13**, 1229–1234.

[89] Kandioler D, Stamatis G, Eberhardt W, Kappel S, Zochbauer-Muller S, Kuhrer I, Mittlbock M, Zwrtek R, Aigner C, Bichler C, et al. (2008). Growing clinical evidence for the interaction of the p53 genotype and response to induction chemotherapy in advanced non-small cell lung cancer. *J Thorac Cardiovasc Surg* **135**, 1036–1041.

[90] Wu ZZ and Chao CC (2010). Knockdown of NAPA using short-hairpin RNA sensitizes cancer cells to cisplatin: implications to overcome chemoresistance. *Biochem Pharmacol* **80**, 827–837.

[91] Hovelmann S, Beckers TL, and Schmidt M (2004). Molecular alterations in apoptotic pathways after PKB/Akt-mediated chemoresistance in NCI H460 cells. *Br J Cancer* **90**, 2370–2377.

[92] Wu ZZ, Sun NK, Chien KY, and Chao CC (2011). Silencing of the SNARE protein NAPA sensitizes cancer cells to cisplatin by inducing ERK1/2 signaling, synoviolin ubiquitination and p53 accumulation. *Biochem Pharmacol* **82**, 1630–1640.

[93] Lin X and Howell SB (2006). DNA mismatch repair and p53 function are major determinants of the rate of development of cisplatin resistance. *Mol Cancer Ther* **5**, 1239–1247.

[94] Hayashi S, Ozaki T, Yoshida K, Hosoda M, Todo S, Akiyama S, and Nakagawara A (2006). p73 and MDM2 confer the resistance of epidermoid carcinoma to cisplatin by blocking p53. *Biochem Biophys Res Commun* **347**, 60–66.

[95] Bauer JA, Kumar B, Cordell KG, Prince ME, Tran HH, Wolf GT, Chepeha DB, Teknos TN, Wang S, Eisbruch A, et al. (2007). Targeting apoptosis to overcome cisplatin resistance: a translational study in head and neck cancer. *Int J Radiat Oncol Biol Phys* **69**, S106–S108.

[96] Wu ZZ, Sun NK, and Chao CC (2011). Knockdown of CITED2 using short-hairpin RNA sensitizes cancer cells to cisplatin through stabilization of p53 and enhancement of p53-dependent apoptosis. *J Cell Physiol* **226**, 2415–2428.

[97] Nadkarni A, Rajesh P, Ruch RJ, and Pittman DL (2009). Cisplatin resistance conferred by the RAD51D (E233G) genetic variant is dependent upon p53 status in human breast carcinoma cell lines. *Mol Carcinog* **48**, 586–591.

[98] Lax SA, Chia MC, Busson P, Klamut HJ, and Liu FF (2001). Adenovirus-p53 gene therapy in human nasopharyngeal carcinoma xenografts. *Radiother Oncol* **61**, 309–312.

[99] Roh JL, Ko JH, Moon SJ, Ryu CH, Choi JY, and Koch WM (2012). The p53-reactivating small-molecule RITA enhances cisplatin-induced cytotoxicity and apoptosis in head and neck cancer. *Cancer Lett* **325**, 35–41.

[100] Li Q, Kawamura K, Yamanaka M, Okamoto S, Yang S, Yamauchi S, Fukamachi T, Kobayashi H, Tada Y, Takiguchi Y, et al. (2012). Upregulated p53 expression activates apoptotic pathways in wild-type p53-bearing mesothelioma and enhances cytotoxicity of cisplatin and pemetrexed. *Cancer Gene Ther* **19**, 218–228.

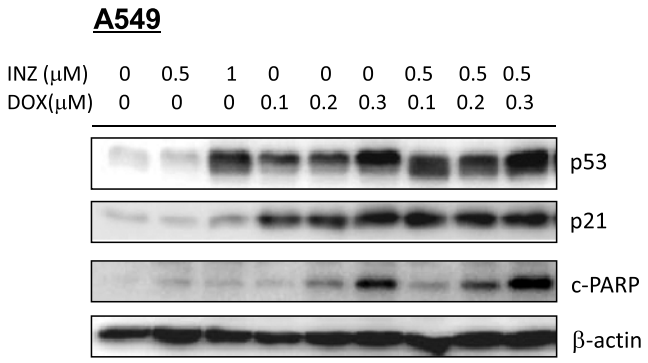

Figure W1. INZ significantly enhances the expression level and activity of p53 as well as the apoptotic response induced by DOX in A549 cells in a dose-dependent manner. Cells were treated with INZ or DOX at the indicated concentrations for 18 hours and harvested for WB analysis. Fifty micrograms of proteins was loaded in each lane, and an anti–β-actin antibody was used to confirm equal loading. Similar results were obtained from three separate experiments.

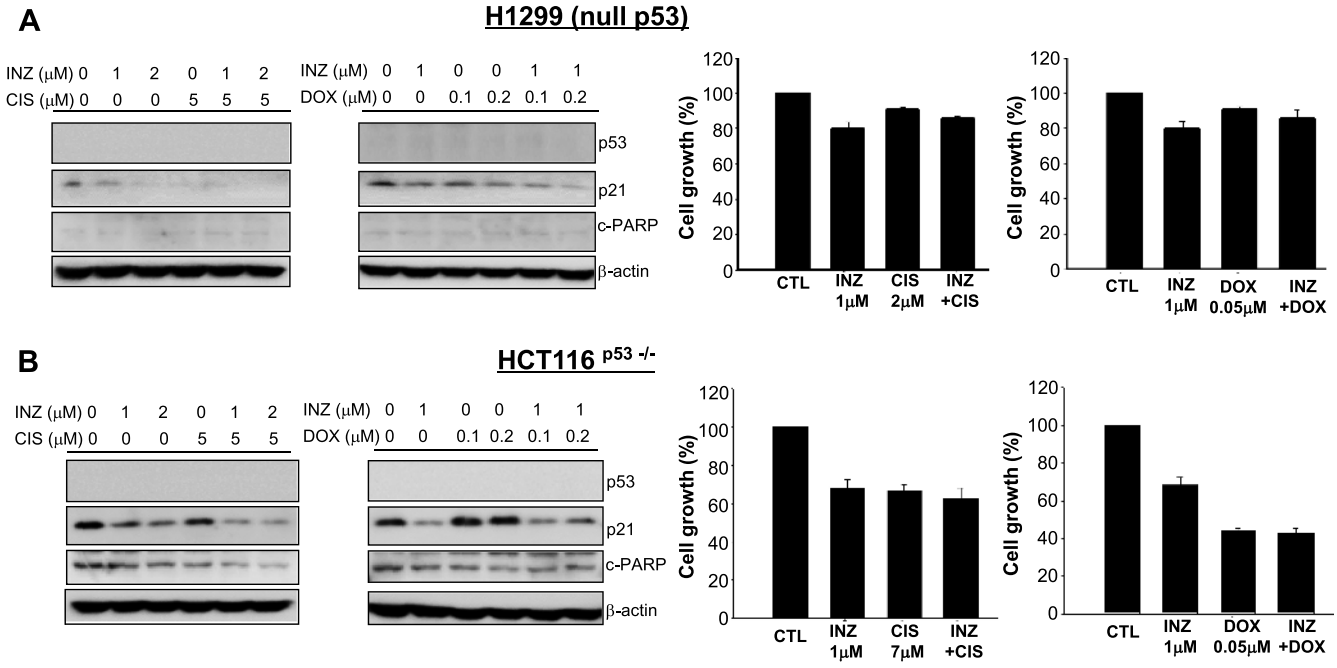

Figure W2. INZ does not enhance the cell apoptotic response and cytotoxicity in the presence of CIS or DOX in p53-null cells. (Left) H1299 (A) and HCT116$^{p53-/-}$ (B) were treated with INZ or/and CIS/DOX at the indicated concentrations for 18 hours and harvested for WB analysis. Fifty micrograms of protein was loaded in each lane, and an anti–β-actin antibody was used to confirm equal loading. Similar results were obtained from three separate experiments. (Right) H1299 (A) and HCT116$^{p53-/-}$ (B) were plated in 96-well plates and treated with INZ or CIS/DOX individually or both simultaneously at the indicated concentrations for 72 hours. Cell viability was determined using the WST cell growth assay. The data shown represent the mean of three independent experiments ± SEM.

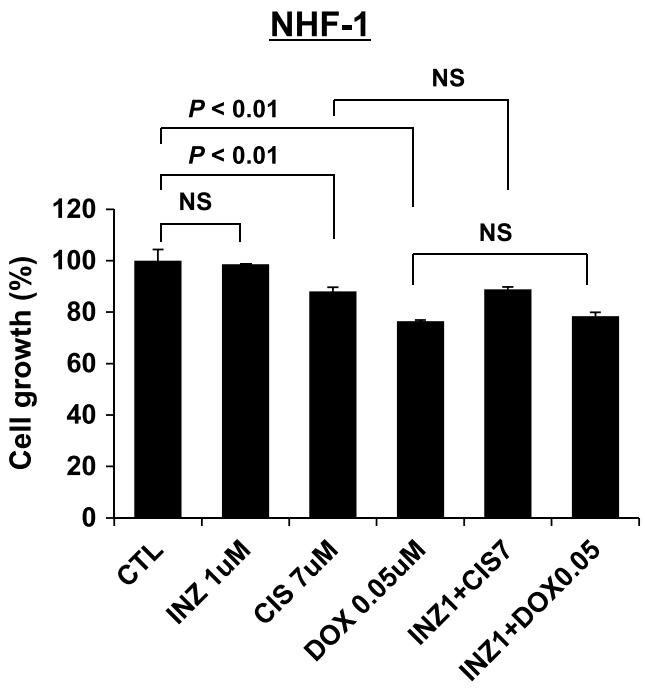

Figure W3. INZ does not enhance the cytotoxic effect of CIS or DOX on NHF-1 cells. NHF-1 cells were plated in 96-well plates and treated with INZ or CIS/DOX individually or both simultaneously at the indicated concentrations for 72 hours. Cell viability was determined using the WST cell growth assay. The data shown represent the mean of three independent experiments ± SEM.